

Solution studies using ^1H NMR^{7,9} and IR^{7,25,26} spectroscopy on Aib-containing peptides of 1-6 residues have suggested that such peptides adopt well-defined structures in solution. A CD study²⁷ on longer peptides (7-19 residues) containing Aib and other (L-) residues reported the helical content of these peptides, but it is not possible to distinguish between 3_{10} or α helices by this method. On the basis of IR studies, C_5 and C_7 hydrogen-bonded ring structures have been suggested^{7,26} as the preferred conformations of several small Aib-containing peptides that are too short to form a 3_{10} -type hydrogen bond. A type II β turn ($\phi_1 = -62^\circ$, $\psi_1 = 137^\circ$, $\phi_2 = 96^\circ$, $\psi_2 = 3^\circ$) was assigned⁷ as the structure of Bu^tCO-Pro-Aib-NHMe; our calculations show that this conformation and the C_5 and C_7 conformations are disallowed for the single Aib residue (Figure 1) and di- and tripeptides (Figures 2 and 3). The minimum appearing in the C_7 region in the energy contour map of the single residue (Figure 1) is 6 kcal/mol higher than that for the 3_{10} conformation, even after minimization with respect to all dihedral angles. It is possible that the hydrogen bonding detected in solutions of small Aib-containing peptides^{7,26} using IR is intermolecular rather than intramolecular. An increase in the number of hydrogen bonds with an increase in the length of the oligopeptide chain in a series of Aib-containing peptides²⁶ was attributed to incipient 3_{10} helices of increasing length. Integrated intensities of the hydrogen bonded N-H stretching band were used to obtain a quantitative estimate of the number of hydrogen bonds.²⁶ The assumption was made, however, that an

$i \rightarrow i - 3$ bond was the only hydrogen bond likely for this molecule; if the possibility of an $i \rightarrow i - 4$ hydrogen bond is admitted, then the same increase in the number of hydrogen bonds for this series of oligopeptides would be expected with incipient α -helix formation, and hence the experiment cannot exclude α -helices.

Stronger evidence for formation of 3_{10} -type ($i \rightarrow i - 3$) hydrogen bonds in small Aib-containing peptides is provided by a ^1H NMR study⁹ on Z-Aib-Pro-Aib-OMe and Z-Aib-Pro-Aib-Ala-OMe. The former molecule is incapable of forming an α -helical hydrogen bond but can form a 3_{10} -type hydrogen bond. The rates of exchange of the various amide and urethane hydrogens in these molecules were measured by monitoring the disappearance of the corresponding proton resonances on addition of D_2O . All but the $\text{H}(\text{N})_{i+2}$ of the tripeptide and the $\text{H}(\text{N})_{i+2}$ and $\text{H}(\text{N})_{i+3}$ of the tetrapeptide exchanged in minutes. These protons took several hours to exchange with deuterium, presumably because they were hydrogen bonded.

Further experimental studies are required to establish whether Aib universally adopts the 3_{10} conformation in solution—as it appears to do in crystal structures. If this is the case, the calculations presented in this study would suggest that the asymmetric geometry that the Aib residue adopts in the crystalline state also prevails in solution.

Acknowledgment. We are indebted to M. S. Pottle for expert advice in computing and Dr. G. D. Smith for making data available to us prior to publication. This work was supported by research grants from the National Science Foundation (PCM79-20279), the National Institute of General Medical Sciences (GM-14312), and the National Institute on Aging (AG-0322) of the National Institutes of Health, U.S. Public Health Service, and by a NATO research grant (No. 1616).

(25) Rao, Ch. P.; Nagaraj, R.; Rao, C. N. R.; Balaram, P. *FEBS Lett.* **1979**, *100*, 244-248.

(26) Rao, Ch. P.; Nagaraj, R.; Rao, C. N. R.; Balaram, P. *Biochemistry* **1980**, *19*, 425-431.

(27) Oekonomopoulos, R.; Jung, G. *Biopolymers* **1980**, *19*, 203-214.

Theoretical Calculations on Proton-Transfer Energetics: Studies of Methanol, Imidazole, Formic Acid, and Methanethiol as Models for the Serine and Cysteine Proteases

Peter A. Kollman* and David M. Hayes

Contribution from the Department of Pharmaceutical Chemistry, School of Pharmacy, University of California, San Francisco, California 94143. Received February 25, 1980

Abstract: We present ab initio calculations on the proton-transfer energetics for models of the serine and cysteine protease "charge-relay systems". The models chosen for these systems include formate...imidazole...methanol and formate...imidazole...methanethiol and the proton-transfer isomers of these complexes. Complete optimization of the monomers and optimization of the molecule-molecule distance in dimeric complexes was carried out with an STO-3G basis set, with single-point calculations on the above trimers. Because of the well-known defects of this basis set in treating ionic molecules, we carried out a number of calculations with the 4-31G basis set. In view of the size of the systems considered, we attempted to model the above complexes at the 4-31G level by using only dimer energy surfaces, with three-body effects determined from the STO-3G and 4-31G calculations on model systems. We then validated this approach with explicit 4-31G calculations on the serine protease trimers. In contrast to previous theoretical calculations, we conclude that Asp 102 in the serine-charge-relay triad is likely to stay unprotonated during catalysis.

The serine proteases enzymes, which catalyze the hydrolysis of amide and ester bonds, have been the subject of many experimental and theoretical studies. One of the most intriguing aspect of these studies is that the enzymes α -chymotrypsin and subtilisin, which have very different primary structures, both have a "charge-relay triad" serine-histidine-aspartate in the active site^{1,2} (see Figure 1). It has been assumed that the mechanism of

catalysis by these enzymes is identical and that this charge-relay triad is what makes the alcoholic oxygen of serine a significantly better nucleophile than it is in aqueous solution.

Papain³ and thiosubtilisin⁴ have also been subjects of many theoretical and experimental studies; these enzymes presumably involve a sulfur as a nucleophile in place of the oxygen. In the

(1) Blow, D. M.; Birkhoff, J. J.; Hartley, B. S. *Nature (London)* **1969**, *221*, 337.

(2) Kraut, J.; Robertus, J.; Birkhoff, J.; Alden, B.; Wilcox, R.; Powers, J. *Cold Spring Harbor Symp. Quant. Biol.* **1971**, *36*, 117.

(3) Drenth, J.; Jansonius, J.; Koekoek, R.; Wolthers, B. *Adv. Protein Chem.* **1971**, *25*, 79.

(4) Alden, R. A.; Wright, C. S.; Westfall, F. C.; Kraut, J. "Structure and Function Relationships of Proteolytic Enzymes"; Desmuelle, P., Neurath, H., Otteson, M., Ed.; Academic Press: New York, 1970; p 173.

Table I. Monomer Energies and Proton Affinities

monomer	total energies, au		proton affinities, kcal/mol		
	STO-3G	4-31G	STO-3G	4-31G	exptl
HCOO ⁻	-185.456 27	-187.900 58	478	357	342 ^a
HCOOH	-186.217 88 ^b	-188.469 96			
imidazole	-221.988 00 ^c	-224.467 47	283	248	(225) ^d
imidazole H ⁺	-222.439 55	-224.860 54			
CH ₃ O ⁻	-112.706 37	-114.217 77	528	407	377 ^e
CH ₃ OH	-113.549 19 ^f	-114.867 14 ^f			
CH ₃ S ⁻	-432.105 76	-436.590 45	496	370	355 ^g
CH ₃ SH	-432.896 08 ^h	-437.180 08 ^h			

^a Yamdagni, R.; Kebarle, P. *J. Am. Chem. Soc.* 1973, 95, 4050. ^b Reference 20. ^c Reference 19, $E_T = -221.987 67$ au. ^d Estimated, see ref 13. ^e McIver, R.; Miller, J. *J. Am. Chem. Soc.* 1974, 96, 4323. ^f Reference 18. ^g Bartmess, J.; Scott, J.; McIver, R. *J. Am. Chem. Soc.* 1979, 101, 5056. ^h Reference 21.

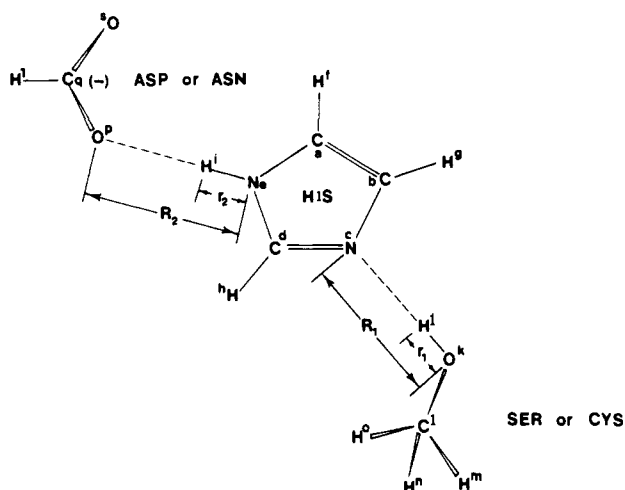


Figure 1. Schematic model of charge-relay triad. In the calculations described in Table II, R_1 or R_2 were optimized by using rigid monomers (Figure 2).

X-ray structure of papain,³ the active site triad is cysteine-histidine-asparagine. In view of the fact that sulfur is an intrinsically better nucleophile than oxygen in aqueous solution, the fact that papain does not have as strong a Lewis base (asparagine instead of aspartate anion) in its active site is reasonable, but recently Angelides and Fink⁵ have suggested that the catalytically active form of papain is not the X-ray conformation but one in which Asp-158 replaces Asn-175 in the charge-relay triad. This also appears to be the structure in the "active site" of thiosubtilisin.

There have been a number of previous theoretical molecular orbital studies of the serine protease mechanism; all, however, used semiempirical molecular orbital theory.⁶⁻⁹ Only Scheiner and Lipscomb⁶ attempted to correct their energy surfaces by calculated energies on smaller model compounds. During the course of this study, studies of the cysteine protease mechanism employing ab initio methods appeared,^{10,11} but these studies did not consider the possible role of Asp in a "cysteine-charge-relay" triad. Thus, one of the goals of this study was to examine the electronic structure and the proton-transfer energetics of serine- and cysteine-charge-relay diads and triads.

Our earlier study of the electrostatic potential in the active site of carboxypeptidase A¹² suggested that it would be of interest to

examine this potential in a variety of enzymes, in order to assess its possible role in catalysis. Thus a second goal of this study was to examine the electrostatic potential and its gradient in the region of the enzyme active site and to compare these properties for subtilisin, papain, and α -chymotrypsin.¹³

In this study, we present ab initio calculations on dimers and trimers which are models of the serine and cysteine protease "charge-relay" enzymes. In particular, we examine dimers and trimers with both the STO-3G and 4-31G basis sets. We estimate the energies of the serine protease model trimer formate...imidazole...methanol and its proton-transfer isomers in the following way: (a) STO-3G calculations on the trimers, (b) STO-3G calculations on the trimers corrected for proton affinity errors, (c) 4-31G calculations on dimers with three-body corrections from model systems, and, finally, (d) explicit 4-31G calculations on the trimers. The latter three approximations are far better than the STO-3G calculations alone, and the results of the calculations, along with calculations on the electrostatic potentials in the active site of the proteins, lead to interesting insights into the first step of catalysis in these enzymes. After we have validated approximations (b) and (c) for the serine protease trimers, we applied these levels of theory to the cysteine protease trimers.

Computational Details

We used our CDC 7600 version of Gaussian 70¹⁴ for most of the quantum mechanical calculations reported in this study, with the exception of the complete geometry optimization of the monomers, where the program AKSCF¹⁵ was used. These ab initio calculations employed both STO-3G¹⁶ and 4-31G basis sets.¹⁷ The electrostatic potential calculations used the program ESPOT, developed at UCSF.¹²

Results

Geometries, Energies, and Proton Affinities of Monomers. The molecules for which complete geometry optimization was carried out by using analytical energy gradients are shown in Figure 2, where the geometries are presented. These optimizations were carried out at the STO-3G level, with single-point calculations at this geometry with the 4-31G basis set. Table I contains the STO-3G and 4-31G energies of the monomers employed in this study as well as calculated and experimental proton affinities.

Previous workers had done complete STO-3G optimization on the neutral molecules CH₃OH,¹⁸ imidazole,¹⁹ formic acid,²⁰ and

- (5) Angelides, K.; Fink, A. L. *Biochemistry* 1979, 18, 2355 and 2363.
 (6) Scheiner, S.; Kleier, D.; Lipscomb, W. *Proc. Natl. Acad. Sci. U.S.A.* 1975, 72, 2606. Scheiner, S.; Lipscomb, W. *Ibid.* 1976, 73, 432.
 (7) Demoulin, D. Ph.D. Thesis, Princeton University, 1976.
 (8) Amidon, G. *J. Theor. Biol.* 1974, 46, 101.
 (9) Umeyama, H.; Imamura, A.; Nagata, C.; Hanano, M. *J. Theor. Biol.* 1973, 41, 485. Umeyama, H. *Chem. Pharm. Bull.* 1974, 22, 2518. Umeyama, H.; Imamura, A.; Nagata, C. *Ibid.* 1975, 23 3075.
 (10) van Duijnen, P.; Thole, B.; Hol, W. *Biophys. J.* 1979, 9, 273. van Duijnen, P.; Thole, B.; Broer, B.; Nieuwpoort, W. *Int. J. Quantum Chem.*, in press.
 (11) Clementi, E. *Int. J. Quantum Chem.* 1980, 17, 651.

- (12) Hayes, D. M.; Kollman, P. *J. Am. Chem. Soc.* 1976, 98, 3335.
 (13) A preliminary report of this study has been completed: Hayes, D. M.; Kollman, P., In "Catalysis in Chemistry and Biochemistry: Theory and Experiment"; Pullman, B., Ed.; D. Reidel, Publishing Co.: Boston, Mass., 1979; p 77.
 (14) This is a modified version of QCPE No. 236: Hehre W. J., et al. *QCPE*, 1973, 11, 236.
 (15) This is an NRCC (National Resource for Computational Chemistry) program developed by A. Komornicki of NASA, Ames, Moffett Field, Calif.
 (16) Hehre, W. J.; Stewart, R. F.; Pople, J. A. *J. Chem. Phys.* 1969, 51, 2657.
 (17) Ditchfield, R.; Newton, M. D.; Hehre, W. J.; Pople, J. A. *J. Chem. Phys.* 1971, 54, 724.

Table II. Calculated Interaction Energies for Charge Transfer and Distances for Dimers

dimer	$R(\text{STO})^a$	$-\Delta E(\text{STO})^b$	Δq^c	$R(4-31G)^d$	$-\Delta E(4-31G)^e$	Δq^c
imidazole-HOCH ₃	2.91	5.86	0.04	2.91	9.24	0.04
imidazole ⁻ OCH ₃	2.30	70.73	0.28	2.48	40.00	0.14
imidazole-HOOCH	2.78	8.71	0.06	2.78	12.27	0.05
imidazole ⁻ OOCH	2.38	47.38	0.20	2.53	27.16	0.10
imidazole-HSCH ₃	3.71	1.36	0.11	3.66	3.61	0.03
imidazole ⁻ SCH ₃	2.80	47.18	0.24	3.08	28.41	0.18
imidazole H ⁺ -OCH ₃	2.23	180.54	0.37	2.43	128.97	0.20
imidazole H ⁺ -SCH ₃	2.67	146.05	0.37	3.00	108.13	0.29
imidazole H ⁺ -OOCH	2.26	148.27	0.30	2.46	110.15	0.15

^a Calculated minimum energy distance for dimers. ^b Calculated interaction energies in kcal/mol. ^c Charge transfer from nucleophile to electrophile. ^d Estimated minimum energy distances for dimers, see text. ^e Calculated interaction energies in kcal/mol.

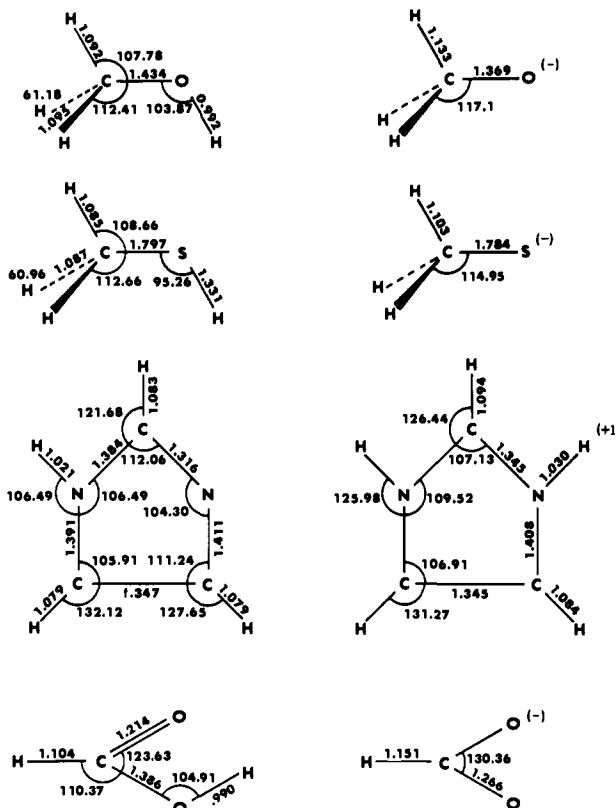


Figure 2. STO-3G optimized geometries of monomers. C_{3v} symmetry was found for CH_3O^- and CH_3S^- , C_{2v} symmetry for ImH^+ and HCOO^- , and C_s symmetry for CH_3OH , CH_3SH , Im , and HCOOH . The large numbers near the hydrogens of CH_3OH and CH_3SH are the dihedral angles for rotation relative to the OH (SH) bond.

methanethiol²¹ by using cyclic optimization methods, and with the exception of imidazole, our results are essentially identical with theirs. The largest difference was found for imidazole, where the gradient optimization finds an energy lower by ~ 0.00033 au than that in ref 19; the ring geometry, however differs by at most 1° in the bond angles.

Potential Surfaces for Dimers and Trimers. (a) **STO-3G Energy Surfaces.** Using STO-3G optimized monomers, we proceeded to optimize the H-bonded distance of the nine dimers relevant to the serine and papain (thiosubtilisin) charge-relay systems. We assumed linear H-bonding geometries and, for the imidazole (or its cation) H-bonding partner, that its plane of symmetry was perpendicular to that of the imidazole. These distances and

Table III. Relative Energies^a for Dimers and Trimers with the STO-3G Basis Set

	uncorrected energy ^b	corrected energy ^c
Dimer		
$\text{Im}\cdots\text{HOCH}_3$	0	0
$\text{ImH}^+\cdots\text{OCH}_3$	68.93	10.34
$\text{Im}\cdots\text{HOOCH}$	0	0
$\text{ImH}^+\cdots\text{OOCH}$	53.38	-1.22
$\text{Im}\cdots\text{HSCH}_3$	0	0
$\text{ImH}^+\cdots\text{SCH}_3$	66.00	13.71
Trimer		
$\text{CH}_3\text{OH}\cdots\text{Im}\cdots\text{OOCH}$	0	0
$\text{CH}_3\text{O}^-\cdots\text{ImH}^+\cdots\text{OOCH}$	53.20	-3.68
$\text{CH}_3\text{O}^-\cdots\text{Im}\cdots\text{HOOCH}$	22.68	22.80
$\text{CH}_3\text{SH}\cdots\text{Im}\cdots\text{OOCH}$	0	0
$\text{CH}_3\text{S}^-\cdots\text{ImH}^+\cdots\text{OOCH}$	42.02	-27.76
$\text{CH}_3\text{S}^-\cdots\text{Im}\cdots\text{HOOCH}$	7.34	18.90

^a Energies in kcal/mol. ^b Direct STO-3G calculations. ^c STO-3G energy corrected for proton affinity error as described in text.

interaction energies, as well as the amount of charge transfer using Mulliken populations, are reported in Table II.

We then carried out STO-3G calculations on the trimers (at the geometries optimized for the dimers), and the results of these calculations are reported in the first column of Table III. These results are similar to previous calculations on the serine protease model employing CNDO/2⁷⁻⁹ and PRDDO⁶ in that these authors⁶⁻⁹ found that the "triple-ion" structure was much higher in energy than the "double-proton-transferred" structure.

Table IV contains the STO-3G Mulliken populations on the serine and cysteine protease model trimers. The close correspondence between the charge transfer found in the trimer and the sum of the dimer charge transfers (in parentheses in Table IV) suggests that the charge redistribution effects in the trimers are well approximated by carrying out calculations on the dimers. Not surprisingly, this approximation is least satisfactory for the strongly interacting "triple-ion" structures.

(b) **Corrected STO-3G Energy Surfaces.** Because it is clear from the data in Table I that the STO-3G basis set does rather poorly in reproducing the relative proton affinities of formate, imidazole, CH_3O^- , and CH_3S^- , we sought a method to correct our relative energies to compensate for this error. In the second column of Table III, we "correct" the STO-3G calculated energies for proton affinity errors in the isolated molecules, making use of the Mulliken populations in an analogous way to Scheiner and Lipscomb.⁶ For example, the STO-3G basis overestimates the proton affinity of CH_3O^- by 151 kcal/mol and the proton affinity of imidazole by 58 kcal/mol. In the optimized structure of $\text{ImH}^+\cdots\text{OCH}_3^-$, we find 0.63 net plus charge on the atoms of ImH^+ and 0.63 net minus charge on the atoms of CH_3O^- . Thus, our corrected energy for proton transfer = $68.93 - 0.63(151 - 58)$ or 10.34 kcal/mol. We can make use of these corrections in the trimer surfaces as well, using the Mulliken populations for charge transfer found in those systems, and these are also reported in Table III.

(18) Lathan, W. A.; Curtiss, L. A.; Hehre, W. J.; Lisle, J. B.; Pople, J. A. *Prog. Phys. Org. Chem.* **1973**, *10*, 175.

(19) Del Bene, J. *J. Am. Chem. Soc.* **1978**, *100*, 5285.

(20) Del Bene, J.; Worth, G. T.; Marchese, F. T.; Conrad, M. E. *Theor. Chim. Acta* **1975**, *36*, 195.

(21) Collins, J. B.; Schleyer, P. v. R.; Binkley, J. S.; Pople, J. A.; *J. Chem. Phys.* **1976**, *64*, 5142.

(22) Bartmess, J. E.; Scott, J. A.; McIver, R. T., Jr. *J. Am. Chem. Soc.* **1979**, *101*, 6056.

Table IV. Net Charges on Trimers (STO-3G Basis Set)^a

trimer	q_1^b	q_2^c	q_3^d
CH ₃ OH...Im...OOCH	-0.05 (-0.04)	-0.16 (-0.16)	-0.79 (-0.80)
CH ₃ O ⁻ ...ImH ⁺ ...OOCH	-0.67 (-0.63)	+0.40 (+0.33)	-0.73 (-0.70)
CH ₃ O ⁻ ...Im...HOOCH	-0.71 (-0.72)	-0.21 (-0.23)	-0.08 (-0.05)
CH ₃ SH...Im...OOCH	-0.01 (-0.01)	-0.20 (-0.19)	-0.79 (-0.80)
CH ₃ S ⁻ ...ImH ⁺ ...OOCH	-0.68 (-0.63)	+0.45 (0.33)	-0.77 (-0.70)
CH ₃ S ⁻ ...Im...HOOCH	-0.75 (-0.76)	-0.18 (-0.19)	-0.07 (-0.05)

^a In parentheses are charges calculated by assuming additivity. ^b Net charge on CH₃OH, CH₃O⁻, CH₃SH, or CH₃S⁻. ^c Net charges on imidazole or protonated imidazole. ^d Net charge on formic acid or formate.

Table V. Analysis of Contributions to the Trimer Interaction Energies^a

molecule	ΔE_1^b	$\frac{\Delta E(A\cdots B) + \Delta E(B\cdots C)^c}{\Delta E(A\cdots C)^d}$	$\Delta E(A\cdots C)^d$	$\Delta E(A\cdots B\cdots C)^e$	relative ΔE_t^f
STO-3G Interaction Energies					
CH ₃ OH...Im...OOCH ⁻	0	-53.24	-0.94	-2.26	0
CH ₃ O ⁻ ...ImH ⁺ ...OOCH ⁻	245.33	-328.81	48.07	32.17	53.20
CH ₃ O ⁻ ...Im...HOOCH	50.92	-79.44	-0.87	-4.37	22.68
CH ₃ SH...Im...OOCH ⁻	0	-48.74	-0.39	-2.05	0
CH ₃ S ⁻ ...ImH ⁺ ...OOCH ⁻	212.41	-294.32	47.23	25.52	42.02
CH ₃ S ⁻ ...Im...HOOCH	18.00	-55.89	-0.58	-5.37	7.34
4-31G Interaction Energies					
CH ₃ OH...Im...OOCH ⁻	0	-36.40	-1.25	-1.89 ^g	0
CH ₃ O ⁻ ...ImH ⁺ ...OOCH ⁻	160.70	-239.12	47.41	18.02 ^g	25.30
CH ₃ O ⁻ ...Im...HOOCH	50.15	-52.27	-0.79	-3.49 ^g	31.89
CH ₃ SH...Im...OOCH ⁻	0	-30.77	-0.93	-3.38 ^g	0
CH ₃ S ⁻ ...ImH ⁺ ...OOCH ⁻	123.23	-218.28	44.71	11.34 ^g	-3.91
CH ₃ S ⁻ ...Im...HOOCH	12.70	-40.68	-0.56	-6.79 ^g	-0.25

^a Energies in kcal/mol. ^b Relative energies of isolated monomers. ^c Sum of two-body interaction energies between H-bonded molecules. ^d Two-body interaction energy between alcohol (or thiol) and acid. ^e Three-body nonadditivity in interaction energy. ^f Relative total energy for the trimer, referenced to the most stable species. ^g These are estimated from the STO-3G values and model calculations, see text.

(c) **4-31G Calculations on Dimers with Corrections to Model Nonadditivity and Long-Range Interactions.** Because of the great difference in the results predicted by the "uncorrected" and "corrected" STO-3G calculations, we sought to carry out 4-31G calculations on these models. As one can see from Table I (see also ref 13), the 4-31G basis makes much smaller errors in the proton affinities for the molecules considered here. These calculations are, however, very time consuming even for dimeric complexes, so we sought an approximation that would allow us to estimate the 4-31G trimer energies on the basis of the dimer calculations and corrections for nonadditivity from smaller model systems.

(1) **4-31G Dimer Surfaces.** First, we carried out 4-31G calculations on the model dimers and these are reported in Table II. The 4-31G distances for the neutral species Im...HOCH₃ and Im...HOOCH were taken directly from the STO-3G calculations since the optimized distance for H₃N...HOH is nearly identical with those for the two basis sets.^{18,23} Since the optimum N...S distance for H₃N...HSH was 3.52 Å (4-31G) and 3.57 Å (STO-3G), the 4-31G distance for Im...HSCH₃ was chosen to be 0.05 Å shorter than that found with the STO-3G basis set.

Model calculations with the STO-3G and 4-31G basis set on H₃NH⁺...OH⁻ and H₃NH⁺...SH⁻ led to the choices for the dimer distances in ImH⁺...OOCH⁻, ImH⁺...OCH₃⁻, and ImH⁺...SCH₃⁻. In H₃NH⁺...OH⁻, the 4-31G calculated N...O distance was 0.20 Å longer than the STO-3G; in H₃NH⁺...SH⁻, the 4-31G calculated N...S distance was 0.33 Å longer than the STO-3G distance. Thus, the 4-31G distances for the three zwitterions were chosen by adding the appropriate distance (0.20 Å for N...O, 0.33 Å for N...S) to the STO-3G optimized value.

For the three ion-neutral systems, the distances were estimated as described for Im...OCH₃⁻. The STO-3G optimized distances for Im...HOCH₃, Im...OCH₃⁻, and ImH⁺...OCH₃⁻ are 2.91, 2.30, and 2.23 Å. Thus, the 4-31G distance for Im...OCH₃⁻ was chosen to be between that of Im...HOCH₃ and that of ImH⁺...OCH₃⁻

Table VI. Relative Energies for Dimers and Trimers with the 4-31G Basis Set^a

dimers	relative energy	dimers	relative energy
Im...HOCH ₃	0	Im...HSCH ₃	0
ImH ⁺ ... ⁻ OCH ₃	34.23	ImH ⁺ ...SCH ₃ ⁻	23.27
Im...HOOCH	0		
ImH ⁺ ...OOCH ⁻	18.76		
trimers		"estimated energy" ^b	directly calcd energy
CH ₃ OH...Im...OOCH ⁻	0	0 ^d	
CH ₃ O ⁻ ...ImH ⁺ ...OOCH ⁻	25.3	27.2 ^e	
CH ₃ O ⁻ ...Im...HOOCH	31.9	34.2 ^f	
CH ₃ SH...Im... ⁻ OOCH	0		
CH ₃ S ⁻ ...ImH ⁺ ... ⁻ OOCH	-3.9		
CH ₃ S ⁻ ...Im...HOOCH	-0.3		

^a In kcal/mol. ^b See Table V and text for description of calculations. ^c Interpolated total energy $E_T = -527.3035$ au. ^d $R_1 = 2.93$ Å; $R_2 = 2.69$ Å. ^e $R_1 = 2.53$ Å, $R_2 = 2.56$ Å. ^f $R_1 = 2.53$ Å, $R_2 = 2.79$ Å.

by the same ratio as found with the STO-3G basis (0.61/0.68) or $R = 2.48$ Å. We tested this approximation for Im...OCH₃⁻ and found that the 4-31G optimized value for this distance was 2.58 Å and the dimerization energy 40.7 kcal/mol rather than the 40.0 kcal/mol found at 2.48 Å. Thus, even though our distance estimates are only approximate, the energy errors involved in making such estimates appear quite small.

(2) **4-31G Calculations to Approximate the Trimer Energies.**

To estimate the energies of the trimers using the 4-31G calculations on the dimers requires two additional sets of information. In a trimer A...B...C, the total interaction energy ΔE is the sum of the two-body energies $\Delta E(A\cdots B)$, $\Delta E(B\cdots C)$, and $\Delta E(A\cdots C)$ and nonadditivity energy $\Delta E(A\cdots B\cdots C)$. The STO-3G values for these quantities are reported in Table V. The data in Table II give us the values for $\Delta E(A\cdots B)$ and $\Delta E(B\cdots C)$ for the 4-31G basis, and we need values for $\Delta E(A\cdots C)$ and $\Delta E(A\cdots B\cdots C)$. Since

(23) Kollman, P.; Johansson, A.; McKelvey, J.; Rothenberg, S. *J. Am. Chem. Soc.* **1975**, *97*, 955. Kollman, P. *J. Am. Chem. Soc.* **1977**, *99*, 4875.

the molecules A and C are rather small, we calculated $\Delta E(A\cdots C)$ directly with the 4-31G basis set and these energies are presented in Table V.

The nonadditivities $\Delta E(A\cdots B\cdots C)$ are more difficult to estimate; here we turn to model calculations. We used the STO-3G nonadditivities on the six trimers (Table V) and carried out calculations on smaller trimers at both the STO-3G and 4-31G level. For example, the nonadditivities in the interaction energy for $\text{HO}\cdots\text{NH}_4^+\cdots\text{OH}^-$ were 35.21 kcal/mol (STO-3G) and 19.72 kcal/mol (4-31G). The STO-3G value is encouragingly close to value of 32.17 kcal/mol found in the corresponding serine protease model trimer and suggests a 4-31G nonadditivity of $19.72/35.21 \times 32.17 = 18.02$ kcal/mol for this trimer. Similar calculations on the other trimers lead to the nonadditivities presented in Table V.²⁴ In each case, we have calculated the STO-3G and 4-31G nonadditivity in the smaller model system (NH_3 and NH_4^+ as models for Im and ImH^+ , OH^- as a model for HCOO^- and CH_3O^- , H_2O as a model for HOCH and CH_3OH , and H_2S and HS^- as models for CH_3SH and SH^-) and used the ratio of the nonadditivities to scale the STO-3G calculated nonadditivity in the protease model trimer.

Finally, in Table VI, we summarize our values for the proton-transfer energetics by the 4-31G basis set: the dimer values are directly calculated; the estimated trimer energies have been determined as described above and in Table V.

(d) **Direct 4-31G Calculations on the Serine Protease Model Trimers.** In order to put the estimates in Table VI on a firmer basis, we carried out 4-31G calculations on the serine protease model trimers, optimizing the distances R_1 and R_2 (for the triple ion, we constrained R_1 and R_2 to change by the same increments, starting with the values of 2.43 and 2.46 Å given in Table II).²⁵ The results are summarized in Table VI and confirm the fact that at the 4-31G level, the triple ion is more stable than the proton-transferred structure. As we have noted, our method of estimating dimer distances and the nonadditivities $\Delta E(A\cdots B\cdots C)$ in section c above are only approximate. It is thus an important validation of this approach that the relative "estimated energies" and directly calculated energies (Table VI) are in such good correspondence.

Discussion

Analysis of the Calculations. The major differences between the calculations reported here and those in our preliminary study¹³ were a complete optimization of monomer geometries, an optimization of H bond distances, and the use of a 4-31G basis set in this study. Other more minor changes involve the use of Mulliken populations here to "modulate" the proton affinity corrections and a correct proton affinity for CH_3S^- (we estimated the previous one and were significantly in error). However, the major conclusion, that the structure $\text{CH}_3\text{O}^-\cdots\text{ImH}^+\cdots\text{OOCH}$ is lower in energy than $\text{CH}_3\text{O}^-\cdots\text{Im}\cdots\text{HCOCH}$, has been strengthened by this study.

(24) We used the STO-3G optimized monomer geometries for NH_4^+ , H_2O , and NH_3 from ref 18 and H_2S from ref 21. For OH^- , the STO-3G-optimized distance is 1.068 Å; for SH^- , this distance is 1.347 Å. At these distances, the energies in atomic units are as follows: OH^- (STO-3G, -74.06520; 4-31G, -75.22599) and SH^- (STO-3G, -393.50578; 4-31G, -397.62302). The 4-31G energy at the STO-3G geometry of H_2S is -398.20300 au. In doing the model trimer (dimer) calculations, we used the distances from Table II (STO-3G distances for the STO-3G model, 4-31G distances for the 4-31G model) and placed the molecules in H-bonding orientations. When NH_4^+ (model for Im) was the central molecule, the two OH^- (or OH^- and SH^-) were placed with each OH^- along one of the N-H bond directions with N-H \cdots O-H linear (the optimized orientation of OH in $\text{NH}_4^+\cdots\text{OH}^-$). Optimization of the N-S-H angle of $\text{NH}_4^+\cdots\text{SH}^-$ led to an angle of 100°; this value was used for SH^- as the electron donor, with the H bisecting the two NH_4^+ (NH_3) hydrogens not involved in the H-bonding network. In the models with NH_3 as the central molecule, the OH^- (SH^-) was placed along a N-H bond, with the external hydrogen placed as above. One OH (SH) bond from H_2O (H_2S) was directed along the lone pair of NH_3 , with the external hydrogen trans to the N-H involved in the H bond with the OH^- (SH^-). With these models, the STO-3G nonadditivities for the six trimers (in the order they appear in Table V) were -6.87, 35.21, -7.51, -2.81, 40.80, and -4.63 kcal/mol and the 4-31G nonadditivities were -5.76, 19.72, -5.99, -4.63, 18.13, and -8.23 kcal/mol.

(25) Each calculation includes 108 basis functions and takes 15 min on a CDC 7600.

Table VII. Electrostatic Potentials^a at Points in Active Site

protein	point (Figure 1)			
	k	c	e	s, p ^b
α -CT ^c	0.08	0.10	0.15	0.235
subtilisin ^c	-0.09	-0.15	-0.18	-0.195
papain ^d	0.28	0.23	0.26	0.33

^a Partial charge in atomic units/Å; conversion factor to kcal/mol = 332. ^b Average of potential at O δ_1 and O δ_2 (O δ and N δ if Asn). ^c Charges of Asp-102, His-57, and Ser-195 removed. ^d Charges of Asn-175, His-159, and Cys-25 removed.

The corrections applied to the calculations based on a STO-3G basis set were large and could be expected to involve large errors. In addition, it is clear that optimization of the intermolecular geometry also accentuates the relative stabilities of ion-pair structures and, in consequence, the corrected proton-transfer energies are underestimated by the STO-3G basis set.

We should note that our previous STO-3G calculations predicted -7 and +5 kcal/mol for the energies of the single and double proton-transferred structures relative to $\text{CH}_3\text{OH}\cdots\text{Im}\cdots\text{OOCH}$ and our current STO-3G estimates (Table IV) predict -4 and 23 kcal/mol for these energies. Both of these results would lead to the physically absurd conclusion that the triple ion will be the intrinsically most stable structure (*more* stable than $\text{CH}_3\text{OH}\cdots\text{Im}\cdots\text{OOCH}$), but both sets of numbers do support the greater stability of the triple ion compared to $\text{CH}_3\text{O}^-\cdots\text{Im}\cdots\text{HCOCH}$, as do the two sets of relative 4-31G energies (Table VI). In fact, the close correspondence between approximation c and the actual 4-31G calculations on the serine protease trimers (Table VI) provides important validation of our calculations on the cysteine protease trimers.

What are the major sources of inaccuracy in these calculations as they might relate to the energetics of the charge-relay system?

It is well established that the 4-31G basis set underestimates the distance and overestimates the interaction energy in intermolecular interactions.²⁶ This overestimate might make the triple-ion structure less stable than we calculate and could be large enough to switch the relative stabilities of the triple-ion and single-ion proton-transferred structures. On the other hand, transfer to a condensed phase, with dielectric constant greater than one, would preferentially stabilize the triple-ion structure through reaction field effects.²⁷ In addition to reaction field effects, specific solvation will stabilize the triple-ion structure. We calculate that two H_2O hydrogen bonds to HCOO^- stabilize it by ~ 29 kcal/mol relative to HCOOH .²⁸ At least two hydrogen bonds to Asp-102 are observed in all the crystal structure of serine proteases² and could significantly stabilize the triple ion relative to the double proton-transferred structure.

The Charge-Relay Triad in the Serine and Sulfhydryl Proteases. All the previous theoretical modeling⁶⁻⁹ of this system has found concerted Ser-195 \rightarrow Asp-102 proton transfer. We feel this is not correct. The reasons why the theoretical calculations have found concerted proton transfer lie in the fact that the methods used greatly overestimated the proton affinity for anions compared with neutral molecules. In our view, only Ser-195 \rightarrow His-57 proton transfer occurs, accompanied by Ser nucleophilic attack on the substrate. On the basis of our calculations, an upper bound for the activation energy for this step is 27 kcal/mol, since the serine can attack the C=O while it is losing its proton, without becoming a "bare" anion.

A charge-relay mechanism suggests either proton or electron motion. Table IV gives the net charge of these changes various species in the serine and sulfhydryl triads. These charges are

(26) Kollman, P.; Kuntz, I. D. *J. Am. Chem. Soc.* **1976**, *98*, 6800.

(27) Beveridge, D.; Schnuelle, G. *J. Phys. Chem.* **1975**, *79*, 2562.

(28) We evaluated the energies of formate-2 H_2O and formic acid- H_2O with the 4-31G basis set (monomers STO-3G geometry optimized^{18,20}). The water O-H bonds approached the O lone pair cis to the COH bond and the other O-H perpendicular to the formate plane. $R(\text{O}\cdots\text{O})$ for formic- H_2O was 2.78 Å; $R(\text{O}\cdots\text{O})$ for formate- H_2O was 2.53 Å. The difference between the H bond energies was 29 kcal/mol, favoring the formate-2 H_2O complex.

similar to those one would calculate from the charge transfer by considering *only* two-body effects (in parentheses), with only ImH^+ in the sulfhydryl triple ion significantly (0.1 e) different from the prediction from two-body charge transfers. The net charges in the 4-31G serine protease triple ion are -0.88 (HCOO^-), $+0.71$ (ImH^+), and -0.83 (CH_3O^-), quite similar to the values of -0.85 , $+0.65$, and -0.80 one would expect from two-body additivity (Table II).

The Role of Protein Electrostatic Potential. We also have calculated the electrostatic potential at the active site of α -chymotrypsin, subtilisin, and papain, removing the partial charges of the active site triad (Asn instead of Asp in the case of papain) from the calculation. Table VII contains these results. As discussed previously,¹³ α -chymotrypsin and subtilisin are sufficiently different, both in the sign of the potential and its gradient across the charge-relay system, to suggest no large "long-range" effects on proton transfer. If proton transfer from Ser is a rate-determining step in catalysis, we would predict that subtilisin, with its potential gradient favoring proton movement from Ser \rightarrow His \rightarrow Asp, would have a larger rate constant than α -chymotrypsin. In α -chymotrypsin, the potential works strongly against His \rightarrow Asp proton transfer by 0.085 au, and in subtilisin, the gradient favors it (Table VII) but by a very small 0.01 au.

The formation of a "bare" CH_3O^- in the enzyme is unlikely to happen, since nucleophilic attack on the substrate is likely to occur as initial proton transfer proceeds. Scheiner and Lipscomb⁶ found, however, that proton transfer was $\sim 90\%$ complete before nucleophilic attack occurred, and this suggests that the calculations reported here might have some relevance to the first stage of catalysis. In any case, the main focus here is on the relative energies of $\text{CH}_3\text{O}^- \cdots \text{ImH}^+ \cdots \text{HCOO}^-$ and $\text{CH}_3\text{O}^- \cdots \text{Im} \cdots \text{HCOOH}$, both of which involve the same CH_3O^- species. To a first approximation, any similar size oxyanion might lead to similar conclusions.

A further consideration in the catalytic action of these proteases is the fact that the proton which is delivered from the serine to histidine needs to be delivered back to the substrate to form the acyl enzyme and release the substrate amine. Thus, any "potential gradient" that the protein sets up to favor serine \rightarrow Histidine charge transfer might at least partially work against proton return to the amine. However, O-H \rightarrow N proton transfer, serine \rightarrow histidine, is intrinsically harder than imidazole $\text{H}^+ \rightarrow \text{NR}-\text{C}(-\text{O}^-)$ proton transfer, such that it is catalytically "favorable" for the protein to speed up the slow rate-determining step at the expense of a reduction of an intrinsically very fast step.

Another interesting feature of these calculations is the difference between the serine and cysteine charge-relay triads. Note in Table VI that all three structures of the cysteine charge-relay triad are comparable in stability. Our calculations on the Cys-His diad, where the ion pair structure is found to be less stable by ~ 23 kcal/mol (Table VI), are similar to those by van Dujnen et al.¹⁰ and Clementi.¹¹ Both of these previous studies and ours¹³ showed that asparagine would stabilize the ion pair by ~ 6 kcal/mol. Significant stabilization of the ion pair could also come from the electrostatic potential gradient (Table VII), which contains an α -helix dipole.¹⁰ The experimental evidence suggests that the ion pair is the catalytically active form of the enzyme.

Thiosubtilisin appears to have a structure-like subtilisin,⁴ with an SH replacing the serine OH. Thus one would clearly expect the triple-ion $\text{CH}_3\text{S}^- \cdots \text{ImH}^+ \cdots \text{OOCH}$ to be the stable structure in its active site. Even in the gas phase, the triple ion is comparable in stability to $\text{CH}_3\text{SH} \cdots \text{Im} \cdots \text{OOCH}$ and the potential gradient and H bonding to Asp in thiosubtilisin should certainly favor $\text{CH}_3\text{SH} \rightarrow \text{Im}$ proton transfer. Why then is thiosubtilisin relatively inactive?⁴ The results in Table VI suggest that this may be due to the double proton-transfer structure now being comparable in stability to the triple ion and, thus, if the proton gets sequestered by the Asp, it cannot catalyze the breakdown of the tetrahedral intermediate. Given the H bonding to Asp⁻ in the protein, however, a more likely explanation is that the proton is held tightly by ImH^+ due both to the presence of Asp⁻ and the electrostatic potential of the protein (Table VII). This suggests

that the relative catalytic inactivity of thiosubtilisin comes from slow *breakdown* of the tetrahedral intermediate. The NHR-(S)C(R')O⁻ group is further from ImH^+ in thiosubtilisin than in subtilisin so that there is less of a tendency for proton transfer. Furthermore, S⁻ being a much better leaving group than O⁻ comes off before the proton is delivered, regenerating the starting material. Philipp, Tsar, and Bender²⁹ have reached similar conclusions regarding the relative inactivity of thiosubtilisin on the basis of kinetic experiments.

The greater activity of papain than subtilisin could come from the substitution of Asn for Asp in the charge relay triad, since Asn would allow ImH^+ to deliver its proton much more easily than Asp⁻. Angelides and Fink, however, suggest that Asp-158 replaces Asn-175 in the catalytically active form of papain. It may be, however, that Asp-158 is not as optimally H bonded to the His as in thiosubtilisin and thus does not inhibit the proton transfer from His \rightarrow tetrahedral intermediate as much as the Asp in thiosubtilisin. The difference in "handedness" of the tetrahedral intermediates in papain and (thiol) subtilisin³⁰ may also contribute to the difference in catalytic efficiency of papain and thiosubtilisin.

Relation to Experiments on the Serine Charge-Relay Systems. There have been a number of studies on the identification of the active site residue responsible for the pK_a near 6.7 in the serine proteases. Hunkapillar et al.³¹ and Koeppel and Stroud³² have suggested that the group responsible for this pK_a is Asp-102; Robillard and Shulman,³³ Markley and Ibanez,³⁴ and Bachovin and Roberts³⁵ interpret their studies to suggest that His-57 is the group responsible for this pK_a .

The above experiments focus on the system $\text{CH}_3\text{OH} \cdots \text{Im} \cdots \text{OOCH}$ and ask the following question: when a proton is added to this triad at a pH near 7, where does it reside? In the absence of substrates, the X-ray evidence suggests that Ser-195 is not H bonding to His-57 at all; in any case, the above pK_a studies focus on the following question: whether, when a proton is delivered, the structure is $\text{ImH}^+ \cdots \text{OOCH}$ or $\text{Im} \cdots \text{HOOCH}$? Our results in Tables VI suggest that, in the gas phase, the neutral form is more stable than the ion pair by 19 kcal/mol. However, our calculations²⁸ on formate- $2\text{H}_2\text{O}$ and formic acid- $2\text{H}_2\text{O}$ suggest that two H bonds can preferentially stabilize formate relative to formic acid by 29 kcal/mol. Thus, we can qualitatively estimate that the ion-pair structure is the more stable one in the enzyme. This is consistent with our detailed study of proton transfer in $\text{H}_3\text{N} \cdots \text{NF} \rightarrow \text{NH}_4^+ \text{F}^-$, where we found that approximately two H_2O were sufficient to stabilize the ion-pair structure.²⁶ In the serine protease enzymes, it appears that there are at least two H bonds to Asp-102, and, thus, our calculations suggest an ion-pair structure. More detailed theoretical calculations by Desmeulles and Allen³⁷ also suggest that the ion-pair structure is more stable than the neutral due to H-bonding stabilization of the ions.

The above experimental and theoretical studies are only directly relevant to the catalytic mechanism if they show an ion-pair structure more stable than neutral. Even if one found $\text{Im} \cdots \text{HOOCH}$ to be more stable than $\text{ImH}^+ \cdots \text{OOCH}$, this does not rule out the fact that, during catalysis and the formation of the incipient nucleophile Ser⁻, the His-Asp ion pair is stabilized relative to the neutral by a large amount (going from a relative stability of +18 (Table V) to -7 kcal/mol (Table VI) in the gas phase.) In the enzyme, with $\epsilon \neq 1$ and the oxyanion further from His,

(29) Philipp, M.; Tsai, I. H.; Bender, M. *Biochemistry* **1979**, *18*, 3769.

(30) Garavito, R. M.; Rossmann, M. G.; Argos, P.; Eventoff, W. *Biochemistry* **1977**, *16*, 5065. This difference in orientation may influence the relative orientation of the lone pairs and the rate of bond cleavage *via* Deslongchamps stereoelectronic effect, according to A. L. Fink (personal communication).

(31) Hunkapillar, M. W.; Smallcombe, S.; Whitaker, D.; Richards, J. H. *Biochemistry* **1973**, *12*, 4732.

(32) Koeppel, R.; Stroud, R. *Biochemistry* **1976**, *15*, 3399.

(33) Robillard, G.; Shulman, R. *J. Mol. Biol.* **1972**, *71*, 507.

(34) Markley, J.; Ibanez, I. *Biochemistry* **1978**, *17*, 4627.

(35) Bachovin, W.; Roberts, J. D. *J. Am. Chem. Soc.* **1978**, *100*, 8041.

(36) Mathews, D. A.; Alden, R. A.; Birktoft, J.; Freer, S.; Kraut, J. *J. Biol. Chem.* **1977**, *252*, 8875.

(37) Desmeulles P. and Allen, L. C., personal communication.

this stabilization will be much smaller than 25 kcal/mol, but it will certainly play some role. Thus, while an identification of the 6.7 pK_a as due to His-57 would, in our opinion, definitively show the triple ion as the relevant species during catalysis, its identification as due to Asp-102 would not rule out the triple ion, since the presence of the incipient serine oxyanion could only change the proton positions in the direction of the triple-ion structure.

Conclusions

The most important conclusion of this paper is that the triple-ion structure is lower in energy than the double proton-transfer structure, even for a simple “gas-phase” model. This is in contrast to the conclusions of previous studies,^{6–9} which found the double proton-transferred structure favored. In fact, our uncorrected STO-3G calculations would conclude similarly to the semi-empirical studies^{6–9} that the double proton-transferred structure is more stable than the triple ion by ~30 kcal/mol. When we correct the STO-3G calculations for proton affinity errors in the monomers, the triple ion is *more* stable by 26 kcal/mol; 4-31G calculations on dimers plus model corrections for nonadditivity find the triple ion *more* stable by 6 kcal/mol, and direct 4-31G trimer calculations find the triple ion *more* stable by 7 kcal/mol.

It is clear that modeling enzyme mechanisms using minimal basis ab initio or semiempirical methods is unreliable unless corrections such as employed here are applied. These corrections are not totally satisfactory (see above) but are superior to uncorrected values. Another, even better, compromise is to use 4-31G ab initio calculations on dimers and simple model systems to estimate nonadditivities in order to calculate the energetics of proton-transfer reactions.

Given that the triple ion and the double proton-transferred structure are of comparable stability in the gas phase, general or

specific solvation effects considered in this paper would further stabilize the triple ion.

Furthermore, it would be an entropic advantage for an enzyme to use only a single proton transfer, rather than requiring the precise alignment of all three residues for concerted proton transfer in its mechanism. This is particularly true since the proton must be delivered back to the substrate before the acyl enzyme can be formed. Thus, our calculations support the view of the enzyme mechanism of ref 33–35 and not those of ref 31 and 32. The use of experimental model systems for “charge-relay” catalysis in aqueous solutions have led to similar conclusions.³⁸

Acknowledgment. We are pleased to acknowledge the NIH (Grant CA-25644) and the NRCC for support of this work. Discussions with Tony Fink, George Kenyon, Wim Hol, Peter Desmeulles, and Lee Allen were essential to the study; Kenyon suggested the subtilisin–chymotrypsin electrostatic potential comparison, Fink suggested the papain conformational change, Hol brought the inactivity of thiosubtilisin to our attention, and we learned from Desmeulles and Allen of their recent calculations on Im^{••}•HCOOH and ImH⁺•••OOCH, which interpret the pK_a of 7 as due to His-57.

(38) G. Rogers and T. C. Bruice, *J. Am. Chem. Soc.* **1974**, *96*, 2473.

(39) Note Added in Proof: A recent study by NaKagawa et al. (*Chem. Pharm. Bull.* **1980**, *28*, 1342), employing a somewhat different geometrical model than that used here and a 431-G basis set, concludes similarly to our previous study¹³ and this work that the “triple ion” is more stable than the “double proton transferred” structure. T. Kosiakoff (personal communication) has shown, using neutron diffraction on DIP inhibited trypsin, that a “triple ion” (Asp⁻ His⁺ >PO₂⁻) rather than a “double proton transferred” (Asp His >PO₂⁻) structure exists in the active site of this enzyme inhibitor complex. This is strong evidence for this type of structure in the transition state of enzyme substrate complexes as well.

Complete Microwave Structure and Electron Distribution for Spiro[2.4]hepta-4,6-diene

Marlin D. Harmony,*† S. N. Mathur,† Jong-In Choe,† Mano Kattija-Ari,† Allison E. Howard,‡ and Stuart W. Staley*†

Contribution from the Departments of Chemistry, University of Kansas, Lawrence, Kansas 66045, and University of Nebraska, Lincoln, Nebraska 68588. Received September 18, 1980

Abstract: Microwave spectra of the normal and seven additional isotopic species of spiro[2.4]hepta-4,6-diene have been observed and analyzed. The resulting rotational constants yield a complete substitution (*r_s*) structure with the following bond lengths: C₁C₂ = 1.494 ± 0.003, C₁C₃ = 1.546 ± 0.003, C₃C₄ = 1.462 ± 0.003, C₄C₅ = 1.361 ± 0.004, C₅C₆ = 1.467 ± 0.003, C₁H₁₂ = 1.079 ± 0.002, C₄H₁₀ = 1.095 ± 0.007, C₅H₈ = 1.080 ± 0.002. Ab initio quantum mechanical calculations at the STO-3G and 6-31G levels have been utilized to describe the electron distribution and to rationalize various experimental results. Both the experimental and the theoretical results provide strong evidence for π-electron donation from the cyclopropyl ring to the cyclopentadiene ring. This π conjugation makes an important contribution to the molecular dipole moment and is the principal factor in determining the changes in C–C bond lengths relative to the parent ring systems.

Introduction

In an earlier communication¹ we presented microwave and theoretical evidence for a conjugative interaction of the cyclopropyl ring with the diene system in spiro[2.4]hepta-4,6-diene (see Figure 1). We report here the complete microwave substitution (*r_s*) structure for this interesting C₇H₈ hydrocarbon and provide further theoretical interpretation of the results. An earlier electron

diffraction structure² is apparently in error, reflecting again the previously encountered difficulty of sorting out similar but inequivalent C–C bond lengths from gas diffraction data. Current work represents a continuation of our fundamental studies of structure and bonding in cyclic systems.^{3,4}

(1) S. W. Staley, A. E. Howard, M. D. Harmony, S. N. Mathur, M. Kattija-Ari, J.-I. Choe, and G. Lind, *J. Am. Chem. Soc.*, **102**, 3639 (1980).

(2) J. F. Chiang and C. F. Wilcox, Jr., *J. Am. Chem. Soc.*, **95**, 2885 (1973).

*University of Kansas.

†University of Nebraska.